Land Cover Changes Implications in Energy Flow and Water Cycle in São Francisco Basin, Brazil, over the Past Seven Decades

Vitor Juste dos Santos (vjustedossantos@gmail.com)
Universidade Federal de Vicosa https://orcid.org/0000-0003-1224-2106
Maria Lúcia Calijuri
Federal University of Vicosa: Universidade Federal de Vicosa
Leonardo Campos de Assis
UNIUBE: Universidade de Uberaba

Research Article

Keywords: Correlation, Flow Rate, Rainfall, Trend Analysis, Water Balance, Water Loss

Posted Date: May 4th, 2021

DOI: https://doi.org/10.21203/rs.3.rs-444119/v1

Abstract

This research aimed to quantify and qualify alterations in land cover and verify the implications of these modifications for variables related to energy flows and water cycle in São Francisco basin (SFB), located entirely in Brazilian territory, in the second half of the 20th century and beginning of the 21st. For this, statistical analyzes (descriptive, trends, seasonal and correlations) were used to quantify changes in the variables of land cover and energy/water flows, in addition to relating them. As a result, it was found that the SFB lost 65,680 km² of native vegetation (10.4% of basin area) to crops and pastures, reducing water infiltration (-52%) while the rains remained stable (-2%). Water loss increased through evapotranspiration (+5%) and surface runoff (+225%). Such changes in the water cycle have entailed an 11% reduction in São Francisco river long term flow rate (Q_{95}), comparing pre and post-1990s period. In SFB, the activities that required water, such as farming activities, are those that promote hydric loss.

Highlights

- Loss of 65,680 km² of native vegetation (10.4% of basin area) to crops and pastures

- Water inflow by rain keeped stable (-2%) and water infiltration was reduced (-52%)

- Water loss increased through evapotranspiration (+5%) and surface runoff (+225%)

- Flow rate of São Francisco river reduced 11%, comparing the pre and post 1990s period

- Activities that need water are those that have been promoting hydric loss in basin

1 Introduction

Investigating Earth's energy and water cycle is essential to understand global climate dynamics and how it impacts and is influenced by human actions (Seyoum and Milewski, 2017; Umair et al., 2019). The terrestrial climate is susceptible to radiation flows, both those of short-wave originating from solar activities and those of long-wave from solar rays' irradiation on the planet's surface (Mokhtari et al., 2018; Yan et al., 2020; Yang et al., 2017).

In addition to the intensity of solar activities, the balance of terrestrial radiation will depend on atmosphere composition, land cover, relief, and the amount of surface water present in the upper lithosphere (Jiang et al., 2021; Mokhtari et al., 2018; Yan et al., 2020). It is already known, therefore, that the energy flux on Earth will depend on the interaction between its various spheres (Atmosphere, Lithosphere, Hydrosphere and Biosphere). It is also known that man, nowadays, can influence these different spheres, changing energy and water flows among them, with their actions that change land cover and atmosphere chemical composition (Rodell et al., 2004; Umair et al., 2019).

Precipitated water will be distinguished into two main categories (Umair et al., 2019): i) first is the demand for water required by the atmosphere, called potential evapotranspiration, which will convert part

of the water present in the lithosphere, hydrosphere and biosphere into real evapotranspiration, not always reaching the total potential demand, as there is dependence on the amount of water present in the environment (Jiang et al., 2021); ii) second is the surface and subsurface runoff, which the balance between these will depend on relief, soils type, land cover, human activities and atmospheric water demand (Ala-aho et al., 2017; Umair et al., 2019). About 67% of the precipitated water across the globe is converted to moisture into the atmosphere by evapotranspiration (Umair et al., 2019).

Although the planet has its dynamics in terms of energy and water flows, human beings, mainly after the industrial revolution (Lindsey, 2009), begin to participate in these complex cycles more significantly. Its activities, such as deforestation, irrigation, urbanization, mining, among others, are vectors of changes in terrestrial land cover and atmospheric chemical composition. In turn, they directly influence energy flows, altering the radiation balance and, consequently, the heat flow (sensitive and latent), which in turn will influence and modify the planet's surface temperature and cause changes in water exchanges between surface and atmosphere (Das et al., 2018; Umair et al., 2019).

To understand these complex interactions between the terrestrial spheres, initiatives emerged, such as the Land Data Assimilation System (LDAS) (https://ldas.gsfc.nasa.gov/). This is developed by the Hydrological Sciences Laboratory of the Goddard Space Flight Center belonging to the National Aeronautics and Space Administration (NASA). With numerical models use, physical processes inherent in the interactions between Earth's surface and atmosphere are modeled from data collected in the field and by orbital images.

From the results, several LDAS projects were developed, which are the Global Land Data Assimilation System (GLDAS), the North American Land Data Assimilation System (NLDAS), the National Climate Assessment - Land Data Assimilation System (NCA-LDAS) and the Famine Early Warning System Network (FEWS NET) Land Data Assimilation System (FLDAS). All of these projects have in common the study and understanding of energy and water terrestrial fluxes, but with different areas and technical specifications with the database used, according to the regional reality.

The use of information generated by models like as LDAS program helps in water resources management, as it is possible to carry out monitoring of drought events, numerical studies of the weather forecast and scientific investigations of water and energy flows (Rodell et al., 2004). Without the application of such models, it would be even more difficult and costly to monitor energy and humidity dynamics with frequent periodicity and adequate geographic scale (Mokhtari et al., 2018; Yang et al., 2017).

Several studies have been carried out based on data generated by LDAS, as the impacts caused by changes in land use and land cover on surface runoff and energy flows, under different climatic conditions, in East Asia (Umair et al., 2019), or to measure water consumption in irrigating crops in agricultural areas in China (Yin et al., 2020). In addition to these, others used data from LDAS to investigate what are the climatic forces associated with occurrences of droughts and wet periods across

the planet (Yuan et al., 2019). There are several other examples of studies, which can be found on LDAS website.

In this context, the objective of this research is to identify and measure changes in the energy flow and water cycle in São Francisco Basin (SFB) in the second half of the 20th century and the first two decades of the 21st, and verifying the implications of land cover modifications, caused by human activities in the last four decades, in changes caused in these cycles' dynamics. Although studies have already been carried out for the basin in this sense, there are still certain gaps concerning changes in the inlet and outlet of water and energy, alterations that have been influenced by human activities.

The most recent SFB studies dealing with the water cycle focus on issues related to water availability and demand. Sun et al. (2016) identified a loss rate of 3.3 km³ of water per year over 13 years of assessment (between 2002 and 2015), caused mainly by the drought that started in 2012 and ended in 2017, which resulted in a loss rate of 27.63 km³ between 2012 and 2015. In this study, data on precipitation and stored water present on the earth's surface were used, and the influence of the *El Niño* phenomenon on drought period occurrence.

In another research, by Koch et al. (2015), water availability and demand were assessed under two scenarios: i) a regionalized world with slow economic development, high population growth and little awareness of environmental problems; ii) a globalized world with low population growth, high growth in Gross National Product (GNP) and environmental sustainability, also adding climate change scenarios to both. As a result, they found that between 2021 and 2050 the basin will be wetter, with more intense rainy and dry periods, and increased water availability for irrigation and a drop in electricity generation.

In addition to these, some other studies highlight that hydroelectric energy production may cease in this first half of the 21st century in drought periods (de Jong et al., 2018). Also the prices of agricultural products generated in SFB will be affected, which will depend on climate change, the production location, variety of products and production technology (Torres et al., 2012). It is as well estimated that economic values of water for use in irrigation tend to increase in the coming decades (Alcoforado de Moraes et al., 2018).

Although they are important researches, none of them deal with implications that changes in land cover, having as vectors the anthropic activities, cause in the energy flows and water cycle in SFB, a theme that will be the focus of this research.

2 Materials And Methods

The stages of this research were organized as follows (Fig. 1): i) study area determination; ii) definition of variables to be studied; iii) statistical analysis of the variables defined in study area over the available historical series; iv) spatiotemporal analysis of the studied variables; v) evaluation of impacts on the water availability in São Francisco River caused by changes in the studied variables.

2.1 Study Area

The São Francisco Basin (SFB) (Fig. 2) is located in the Northeast and North of the Southeast of Brazil, with an area of 630,000 km² and with its main river running 3,200 km from the source, in the State of Minas Gerais, at its mouth, on the border of the States of Alagoas and Sergipe, flowing into South Atlantic Ocean (Bezerra et al., 2019; de Jong et al., 2018). It is between the latitudes of 21º and 7º South, with climatic characteristics, according to the revised classification of Thornthwaite (Feddema, 2005), ranging from humid and wet sub-humid types between latitudes 21º and 10º South (29% of basin area), until dry sub-humid, semi-arid and arid types between latitudes 17º and 7º South (71%).

In humid and wet sub-humid areas, south and southwest of basin, temperatures reach an average of 20ºC (Torres et al., 2012), with potential evapotranspiration ranging from 1,241 to 4,344 mm/year, with an average of 2,300 mm/year (Beaudoing and Rodell, 2019), and rains precipitate an average of 1,500 to 2,000 mm/year (Koch et al., 2015; Sun et al., 2016). In dry sub-humid, semi-arid and arid areas, north and northeast of basin, temperatures reach an average of 26.5ºC (Torres et al., 2012), with potential evapotranspiration ranging from 1,533 to 5,110 mm/year, with an average of 2,884 mm/year (Beaudoing and Rodell, 2019), and rainfall precipitates an average of 350 mm/year (Koch et al., 2015; Sun et al., 2016).

Precipitation in humid and wet sub-humid areas is mainly associated with the South Atlantic Convergence Zone (SACZ) that operates in the southeastern region of Brazil and southwestern Bahia during the summer (between October and March) (Torres et al., 2012). In the dry sub-humid, semi-arid and arid areas, rains are concentrated during the months of March and April, caused mainly by action of the Intertropical Convergence Zone (ITCZ), which acts more intensely in this period due to weakening of the inter-hemispheric south gradient of sea surface temperature, which allows ITCZ to reach regions further south. In the rest of the year, there is a strong presence of a high-level cyclone over the Amazon, which inhibits rains formations in the region and favors dry weather conditions, which is often enhanced by strong *El Niño* events.

The humid and wet sub-humid areas cover almost all the sub-regions of Upper São Francisco and western part of the Middle. The main river has its contribution mainly from these areas, which were responsible for 93%, between 1951 and 1999, of total permanence flow curves (Q_{95}). That is, approximately 43% of basin was responsible for maintaining flow rate that flowed through the riverbed 95% of the time. The other 57%, corresponding to the sub-regions of Low, Lower-Middle, and eastern part of the Middle São Francisco, which are mostly covered by dry sub-humid, semi-arid and arid areas, contributed with remaining 7% of Q_{95} (Pereira et al., 2007; Pruski et al., 2004). This showing the importance of the areas closest to its source for maintenance of main river.

São Francisco has an average flow rate of 2,850 m³/s, ranging from 1,077 to 5,290 m³/s (Bezerra et al., 2019), with a permanence flow curve (Q_{95}) of 800.4 m³/s (Pereira et al., 2007; Pruski et al., 2004). It comes from 70% of the surface waters of entire Northeast region of Brazil (Torres et al., 2012), which has

a population of over 53 million people, approximately a quarter of the Brazilian population. Besides, hydroelectric system of this river normally meets 70% of the demand for electricity in Northeast region (de Jong et al., 2018).

Added to these hydrological conditions, the basin has vegetations of Cerrado types (Savannah Formation) with a great diversity of tree vegetations (Forest Formation) in Upper and western sub-region of Middle São Francisco, as well as the vegetation of Caatinga biome, which is widely spaced and smaller, associated with drier and hotter climate in Low, Lower-Middle and east of Middle São Francisco (Creech et al., 2015).

Land use is predominantly agricultural, with crops (46%) and pastures (41%) dominating the land cover in basin. Aside from, there are remnants of large and medium-sized tree vegetation, urban areas, mining, among others. The main agricultural production is soy, with other major crops such as corn, wheat and cotton, in addition to important fruit centers (Juazeiro and Petrolina) (Correia et al., 2001) and family farming throughout the basin. Vegetations, crops and pastures are on soils of latosol (41% of the basin), podzols (11%), sandy soils (10%) and cambisols (7%) (Alcoforado de Moraes et al., 2018; Creech et al., 2015; Torres et al., 2012).

Covering approximately 7.5% of the Brazilian territory, SFB has a population of over 17 million people (8% of Brazilian population), 21% of which are considered poor by the country's standards (Sun et al., 2016). Due to population growth and the demand for food, water, jobs and services, the municipalities in basin have had satisfactory socio-economic development in recent decades, but at the cost of natural resources, mainly native vegetation, soil and water, relative with deforestation problems, desertification, water scarcity, pollution and water bodies silting up (Creech et al., 2015; de Jong et al., 2018; Koch et al., 2015).

From the above, it is clear that SFB has significant physical-natural and socioeconomic diversity, which are dynamic in space and time. Due to these factors, the basin was defined as a study area precisely because of its dynamics and diversity related to environmental and human aspects, which interfere with each other. The choice focused on dynamics pertinent to energy and water cycles, which are affected by the basin's socio-economic activities, but also affect them. The option for the area is also linked to the fact that the basin has one of the main rivers in Brazil, entirely within the national territory, which passes through the driest region and one of the poorest in the country. The river has great national importance due to its strong potential for economic use, mainly linked to agricultural activities, irrigation, public supply, navigation and generation of electric energy, but has been under strong pressure exactly by exploration of these same activities.

2.2 Variables Definition

The variables defined in this research were those related to the energy flow and water cycle in SFB, as well as those that can interfere in these cycles, referring to land use and land cover, in addition to the minimum, average and maximum flows rate of São Francisco river (Table 1). The GLDAS database units

have been converted, as suggested on Land Data Assimilation System website (https://ldas.gsfc.nasa.gov/faq/ldas), for better comparison between variables.

Table 1
Database used

GLDAS (1948–2019) [https://ldas.gsfc.nasa.gov/gldas]			**Dataset Units**	**Converted Units**
Swnet		Shortwave Radiation Flow	W/m²	W/m²
Lwnet		Long Wave Radiation Flow	W/m²	W/m²
Qh		Sensitive Heat Flow	W/m²	W/m²
Qle		Latent Heat Flow	W/m²	W/m²
Rainf		Rainfall Rate	Kg/m²/s	mm
AvgSurfT		Average Surface Temperature	K	ºC
PotEvap		Potential Evapotranspiration	W/m²	mm
Evap		Real Evapotranspiration	Kg/m²/s	mm
Tveg		Vegetation Transpiration	W/m²	mm
Ecanop		Direct Evaporation of Plants Canopy	W/m²	mm
Esoil		Direct Evaporation of Bare Soil	W/m²	mm
Canint		Moisture in Plants Canopy	Kg/m²	mm
RootMoist		Root Zone Soil Moisture	Kg/m²	mm
Qs		Surface Runoff	Kg/m²/3h	mm
Qsb		Subsurface Runoff	Kg/m²/3h	mm
MapBiomas (1985–2018) [https://mapbiomas.org/]			**Dataset Units**	**Converted Units**
LULC		Lan Use and Land Cover	-	-
MEaSUREs [https://lpdaac.usgs.gov/data/get-started-data/collection-overview/measures/]			**Dataset Units**	**Converted Units**
VCF	**Tree Cover**	Percent Tree Cover (1982–2014)	%	%
	Non-Tree Cover	Percent Non-Tree Cover (1982–2014)	%	%
	Bare Ground	Percent Bare Ground (1982–2014)	%	%
VIP	**NDVI**	Normalized Difference Vegetation Index (1981–2019)	-	-

GLDAS (1948–2019) [https://ldas.gsfc.nasa.gov/gldas]		Dataset Units	Converted Units
ANA (1928–2019) [http://www.snirh.gov.br/hidroweb/]		Dataset Units	Converted Units
Flow Rate	Minimum, Average and Maximum Flows Rate	m³/s	m³/s

The Global Land Data Assimilation System (GLDAS) is a program from the National Aeronautics and Space Administration (NASA) in which observational data from orbital images and information collected in the field are used to model the dynamics of terrestrial phenomena linked to energy flow and the water cycle of the planet Earth. Produces results almost in real-time, with resolutions that vary between 2.5º and 1 km, with historical series between 1948 until today with periodic update (Beaudoing and Rodell, 2019; Rodell et al., 2004).

The data used in GLDAS contains relief information, soil types, vegetation and atmospheric variables such as rain and radiation flows. Data assimilation techniques are employed to incorporate hydrological products based on satellite sensor imaging that include snow cover and water equivalent, soil moisture, surface temperature and leaf area indexes (Beaudoing and Rodell, 2019; Rodell et al., 2004).

The Annual Mapping of Land Use and Land Cover in Brazil (MapBiomas) (Souza et al., 2020) is a collaborative network with specialists in Brazilian biomes, land uses, remote sensing, geographic information systems and computer science, which uses cloud processing and automatic classifiers (Random Forest) developed and operated from Google Earth Engine platform. Since its foundation (2015) it has been generating an annual historical series of land use and land cover maps for the whole of Brazil (1985 to 2018 - Collection 4.1), with a spatial resolution of 30 meters using the series of images from Landsat sensors.

The program Making Earth System Data Records for Use in Research Environments (MEaSUREs), from NASA's Land Processes Distributed Active Archive Center (LP DACC), is dedicated to the advancement of remote sensing and the scientific use of measurements from satellite sensors to expand the understanding of terrestrial system, with production and recording of consistent, high quality and long-term data. Among several databases, those used in this research were the Vegetation Continuous Fields (VCF) (Hansen and Song, 2018) and the Vegetation Index and Phenology (VIP) (Didan and Barreto, 2016). The first is a collection that provides global vegetation information from the Advanced Very High-Resolution Radiometer (AVHRR) long-term records between 1982 and 2014, annually, with a spatial resolution of 5,600 m containing information on the percentage of tree vegetation cover, non-tree vegetation cover and bare ground. The second is another collection containing a monthly historical series from 1981 to 2019, of vegetation and landscape phenology indexes, based on data from the Moderate-Resolution Imaging Spectroradiometer (MODIS), AVHRR and *Satellite Pour l'Observation de la Terre* (SPOT), also with a spatial resolution of 5,600 m.

The Hidroweb Portal (http://www.snirh.gov.br/hidroweb/) is a Brazilian tool that is part of the National Water Resources Information System (SNIRH, acronym in Portuguese) and offers access to database that contains all information collected by the National Hydrometeorological Network (RHN, acronym in Portuguese), which gathers data on flows rate, river height, rainfall, climatology, sediment and water quality. The data used come from conventional fluviometric stations with codes 45298000 (14.3º S and 43.76º W) and 49705000 (10.21 S and 38.82 W), with historical series of daily and monthly frequencies between 1928–2019 and 1959–2019, respectively. The use of these two stations is better detailed in item 3.1, as the choice of both was defined based on some results of this research.

2.3 Statistical Analysis

The statistical procedures were broken down into three stages: i) first performed on variables related to energy flow and water cycle; ii) later on variables related to land use and land cover; iii) and, finally, in the variables related to São Francisco river flow rate and its correlations with the analysis of the previous data.

2.3.1 Statistical analysis on variables related to energy and water cycles

First, the Mann-Kendall test (MK tau) was performed on variables related to energy flow and water cycle, from GLDAS database, monthly, between January 1948 and December 2019.

This first analysis aimed to verify the spatiotemporal behavior of the variables and to search for different trend patterns throughout SFB in the mappings made by the test, pixel by pixel, using the Series Trend tool of the Earth Trend Modeler module available by Idrisi Selva 17.0 software (Eastman, 2016). With the identification of patterns, it was decided to divide the study area into two parts (P1 and P2). This decision is explained in results.

MK tau is a non-parametric trend indicator that measures the degree to which a trend is increasing or decreasing consistently. It was first proposed by Mann (1945) and later studied by Kendall (1975), then enhanced by Hirsch et al. (1982) and Hirsch & Slack (1984), which made it possible to take seasonality into account. It has a range of -1 to + 1. A value of + 1 indicates a trend that continually increases and never decreases. The opposite is true when it has a value of -1. The zero value indicates that there is no consistent trend. All combinations of pair values over time are evaluated at each pixel and a count is made of the number that is increasing or decreasing over time. It is simply the relative frequency of increases minus the relative frequency of decreases (Eastman, 2016).

With P1 and P2 discriminated, descriptive statistics were made to verify variations of the average values of each variable in both areas, checking if in general there was an increase, stability or decrease in each one of them. Stationarity (KPSS) and homogeneity (Pettitt and Buishand) tests were also performed.

The stationarity test used was the KPSS (Kwiatkowski et al., 1992), which allows to check whether a series is stationary or not. The test result varies from zero to ∞ (Eta Observed Value), in which the higher the critical value (Eta Critical Value), greater the tendency for the series not to be stationary, and the opposite being also true, that is, as closer to zero and below the critical value, greater the tendency to stationarity.

The homogeneity tests used were those by Buishand (1982) and Pettitt (1979), that check if a series is homogeneous over time, or if there is a moment when a change or break in that homogeneity occurs. Such tests were selected based on different sensitivities they present for identification at the change time and because they are widely used to test homogeneity in environmental data series (Bickici Arikan and Kahya, 2019; Rougé et al., 2013; Serinaldi et al., 2018; Serinaldi and Kilsby, 2015; Yozgatligil and Yazici, 2016).

2.3.2 Statistical analysis on variables related to LULC and MEaSUREs

To measure changes in land use and land cover in SFB, the Change Analysis tool of Land Change Modeler module, from Idrisi Selva 17.0 software, was used (Eastman, 2016). In this tool, it was possible to verify the main changes between the years 1985 and 2018.

In addition to measuring changes in land use and land cover using MapBiomas data, the MEaSUREs database was also used, which contains data on the percentage of tree cover, non-tree cover and bare ground (VCF) between 1982 and 2014, and NDVI (VIP) between 1981 and 2019, respectively (Didan and Barreto, 2016; Hansen and Song, 2018).

For MapBiomas land use and land cover data, from the measurements generated in Land Change Modeler module, all classes related to human actions (Farming, Mining, Planted Forest and Urban Areas) were grouped into a single class called Anthropogenic Disorders. In this, Mann-Kendall and homogeneity tests (Pettitt and Buishand) were performed.

In the MEaSUREs data, Mann-Kendall test was used to identify differences spatiotemporal trends in the SFB with Series Trend tool of Earth Trend Modeler module from Idrisi Selva 17.0 software aid (Eastman, 2016).

2.3.3 Statistical analysis on variables related to São Francisco river flow rate

The data series on the minimum, average and maximum flows rate of São Francisco river was analysed in two river stations, one located in P1 (code 45298000) and another in P2 (code 49705000).

Mann-Kendall, stationarity and homogeneity tests were also applied. After the application of this tests and results obtained, these were compared to the results of tests related to the variables of previous topics. This was performed to verify possible implications of changes in land cover, in energy flows and,

consequently, in water cycle basin, and the impacts of these processes on flow rate dynamics of São Francisco river at P1 and P2.

To reinforce possible influences of changes in land cover in water cycle basin, correlation analyzes between NDVI and variations related to water cycle were performed, with the aid of Correlate module of Idrisi Selva 17.0 software (Eastman, 2016). The main application of the module is to identify areas that correlate with a specific temporal pattern of interest, calculating the correlation coefficient R between one or more predictors (independent) with a time series of images (dependent) for each pixel. In addition, such analyzes were also performed between historical series of average flows rate in P1 and P2 with rainfall, surface and subsurface runoff data, using Pearson's correlation (Barber et al., 2020).

4 Results And Discussion

This topic is divided into three subtopics, which are: 1) results related to spatiotemporal analysis of energy flow and water cycle variables; 2) results related to spatiotemporal analyzes of land use and land cover and; 3) results and discussion referring to consequences on the dynamics of São Francisco river flow rate resulting from changes in the variables evaluated in the two previous subtopics.

4.1 Spatiotemporal analysis of energy flow and water cycle variables

Mann-Kendall tests carried out for energy flow variables showed that there were different intensities in trends, positive and negative, of radiation flows (short and long waves) and heat (sensitive and latent), in specific areas in SFB between January 1948 and December 2019 (Fig. 3).

Due to this distinctions, the basin was segmented into two parts, P1 and P2 (Fig. 3). Such segmentation was based on trends of radiation flows (short and long waves) (Tables 2 and 3), which will influence the dynamics of other variables, such as heat flows (sensitive and latent), evapotranspiration and presence of moisture in the canopies and plants root zones. These results also guided the choice for used fluviometric stations locations, aiming to relate the changes in trends of the variables evaluated in GLDAS database with flow rate dynamics. The definition of the fluviometric stations followed two conditions: i) close to the place further downstream from P1 and P2, seeking to cover the entire contribution basin and; ii) with sufficient historical series to satisfactorily cover the period of GLDAS and MEaSUREs data.

Table 2
Trend (MK) range values and significance (p) analyze for energy flow variables in P1.

Variable	MK Tau	Area (%)	p-value	Area (%)
Swnet	0.03 to 0.18	95	0	89
	0.18 to 0.41	5	> 0	11
Lwnet	0 to 0.1	10	0	98
	0.1 to 0.33	90	> 0	2
Qh	0.06 to 0.1	2	0	100
	0.1 to 0.4	98	> 0	0
Qle	-0.04 to 0.1	54	0	79
	0.1 to 0.21	46	> 0	21

Table 3
Trend (MK) range values and significance (p) analyze for energy flow variables in P2.

Variable	MK Tau	Area (%)	p-value	Area (%)
Swnet	0.13 to 0.18	9	0	100
	0.18 to 0.41	91	> 0	0
Lwnet	-0.14 to 0.1	42	0	79
	0.1 to 0.33	58	> 0	21
Qh	0.14 to 0.18	4	0	100
	0.18 to 0.4	96	> 0	0
Qle	-0.28 to 0.1	81	0	54
	0.1 to 0.21	19	> 0	46

In P1, the predominant trend was from stability to a slight increase in short-wave radiation flow, from 188 to 198 W/m². Regarding long-wave radiation flow, the predominant trend was a slight to moderate increase, from − 70 to -64 W/m². Sensitive heat flow also had a predominant tendency to grow from light to moderate, from 49 to 63 W/m². Regarding the latent heat flow, there was a predominantly stable tendency for light growth, from 66 to 71 W/m².

In P2, the predominant trend was for a slight to moderate increase in short-wave radiation flow, from 193 to 216 W/m². Regarding long-wave radiation flow, the predominant trend was stability, ranging from − 76

to -73 W/m². The predominant trend of sensitive heat flow was moderate growth, from 65 to 91 W/m². Regarding the latent heat flow, there was a predominantly stability trend, from 51 to 53 W/m².

Even though there are specific cases of mild negative trends, in general, variables related to radiation and heat flows have positive trends in SFB, in both areas (P1 and P2) (Table 4).

Table 4
– Absolute and relative variations of SFB radiation and heat flow.

Variable	Average Variation - P1		Average Variation - P2	
	Absolute	Relative	Absolute	Relative
Swnet	+ 10 W/m²	+ 5%	+ 23 W/m²	+ 12%
Lwnet	+ 6 W/m²	+ 9%	+ 3 W/m²	+ 4%
Qh	+ 14 W/m²	+ 29%	+ 26 W/m²	+ 40%
Qle	+ 5 W/m²	+ 12%	+ 2 W/m²	+ 4%

This fact contributes to positive trends of potential evapotranspiration throughout the basin, notably in P2, influenced by significant positive flow of short-wave radiation and specific heat. Even though the potential evapotranspiration has increased considerably, the real evapotranspiration, although it has grown, has not followed it (Table 5).

Table 5
– Absolute and relative average variations of potential and real evapotranspiration in SFB.

Variable	Average Variation - P1		Average Variation - P2	
	Absolute	Relative	Absolute	Relative
PotEvap	+ 467 mm/year	+ 23%	+ 1072 mm/year	+ 45%
Evap	+ 66 mm/year	+ 8%	+ 31 mm/year	+ 5%

In P1, the average potential evapotranspiration increased from 2,043 to 2,510 mm/year, while average real evapotranspiration increased from 820 to 883 mm/year. In P2, the average potential evapotranspiration increased from 2,359 to 3,431 mm/year, while average real evapotranspiration increased from 631 to 662 mm/year. This is shown in the trend analysis (MK) results, where for potential evapotranspiration, they were 0.175 and 0.309, P1 and P2 respectively. As for the real evapotranspiration, they were 0.04 and zero, P1 and P2 respectively.

While there was an increase in potential and real evapotranspiration, pluviometric indexes remained stable (Table 6).

In P1 the average rainfall decreased from 1.324 to 1.261 mm/year, and in P2 there was no variation in the average, remaining at 694 mm/year. The Mann-Kendall analysis confirms such variations, in P1 with a result equal to zero and in P2 equal to 0.005, that is, a tendency to stability.

If on average the rainfall rates were stable, which led to an increase in real evapotranspiration in P1 and P2, even if not following the potential evapotranspiration, it was the increase in vegetation transpiration (Table 7), which increased in P1 from 265 to 441 mm/year, and in P2 from 290 to 366 mm/year.

Table 7
– Absolute and relative variations in transpiration/evaporation from different sources in SFB.

Variable	Average Variation - P1		Average Variation - P2	
	Absolute	Relative	Absolute	Relative
Tveg	+ 176 mm/year	+ 66%	+ 76 mm/year	+ 26%
Ecanop	− 127 mm/year	− 37%	− 63 mm/year	− 28%
Esoil	+ 13 mm/year	+ 6%	0 mm/year	0%

This increase in transpiration was accompanied by a tendency towards stability with a small increase in water evaporation directly from bare soil and a reduction in the plants' canopies evaporation. In P1, there was a tendency for a small increase in bare soil direct evaporation, from 227 to 240 mm/year, and a tendency for a decrease in plant' canopy direct evaporation, from 341 to 214 mm/year. In P2, there was a tendency to stability in bare soil direct evaporation, remaining at 139 mm/year, and again a tendency to decrease in plant' canopy direct evaporation, from 227 to 164 mm/year.

The increase in evapotranspiration was accompanied by a reduction in the presence of water accumulated in plants' canopies and a decrease in soil moisture in the root zone (Table 8). In P1, there was a water dip in plants' canopies from 0.19 to 0.12 mm, and a decrease in soil moisture in root zone from 244 to 228 mm. In P2, there was a water dip in plants' canopies from 0.11 to 0.07 mm, and a decrease in soil moisture in root zone from 210 to 179 mm.

Table 8
– Absolute and relative average variations in the presence of moisture in canopies and root zone of plants in SFB.

Variable	Average Variation - P1		Average Variation - P2	
	Absolute	Relative	Absolute	Relative
CanopInt	− 0.07 mm	− 37%	− 0.04 mm	− 36%
RootMoinst	− 16 mm	− 7%	− 31 mm	− 15%

Additionally, there was an increase in surface runoff and a decrease in subsurface runoff (Table 9). In P1, there was an increase in surface runoff from 16 to 80 mm/year and a decrease in subsurface runoff from

445.6 to 283.2 mm/year. In P2, there was an increase in surface runoff from 0.8 to 38.4 mm/year, and a drop in subsurface runoff from 126.4 to 38.4 mm/year.

Table 9
Absolute and relative average variations of surface and subsurface runoff in SFB.

Variable	Average Variation - P1		Average Variation - P2	
	Absolute	Relative	Absolute	Relative
Qs	+ 64 mm/year	+ 400%	+ 37.6 mm/year	+ 4,700%
Qsb	− 162.4 mm/year	− 36%	− 88 mm/year	− 70%

Figure 4 shows in general how the trends of each variable from energy flow and water cycle behaved over the period evaluated. The results in Mann-Kendall test show that there were increases in heat and radiation flows across SFB, although on average the latent heat flow is stable at P2, in addition to stability in rainfall indexes. The KPSS test confirms such trends, showing that rainfall has a stationary behavior, both in P1 and in P2, over time, whereas for radiation and heat flows the critical value has been reaching, mainly for specific heat and short-wave radiation, showing a tendency towards non-stationarity throughout the series.

As a consequence of increase in radiation and heat flows, trends in potential and real evapotranspiration are positive, except for real evapotranspiration in P2, tending to stationarity.

Although actual evapotranspiration did not keep up with the increase in potential, it was positive due to the plant transpiration growth, as the water evaporation directly from plants' canopies reduced, and evaporation directly from bare soils was stable. Even though in P2 the KPSS test points out that there is no stationarity in the series, with a possible reduction.

The trends for the presence of moisture in plants' canopies and their root zones are decreasing, ratified by non-stationarity in KPSS test. The reduction in humidity in these places is probably due to the increase in evapotranspiration, but, mainly, to the rise in surface runoff, which has a positive tendency, and to subsurface runoff reduction, which has a downward trend. This shows less water infiltration in the soil, providing less moisture to plants' roots, and less water containment by vegetation, reflected by less water maintenance in their canopies and increase in water loss due to surface runoff.

All variables that showed a trend, positive or negative, with significant p-values, obtained results in Pettitt and Buishand tests that showed a break in homogeneity mainly in the 1990s, varying between 1995 and 2000 in P1, and between 1986 and 2000 in P2. The variables latent heat, precipitation, evapotranspiration, direct water evaporation from bare soil and subsurface runoff, whether in P1 and P2 or one of them, were those that obtained meanings that were more distant from zero, being exactly those that showed a break in homogeneity in different years to the rest of variables. This means that there was no break in their series, as the results in Mann-Kendall and KPSS tests showed that the variables with

most distant values of significance were exactly those with no defined trend, that is, tending to stationarity.

4.2 Spatiotemporal analyzes of land use and land cover

Between 1985 and 2018 at SFB there was a reduction of 68,631 km² of native vegetation formations, equivalent to 10.8% of the basin total area. From this reduction, 95.7% was caused by agricultural activities (perennial and semi-perennial crops, planted forests and pastures), and the remainder, 2,951 km² (4.3%), due to the advance of urban areas, mining and other uses (Fig. 5). The most degraded vegetation formations were savannas and grasslands, medium and small sizes vegetations from Cerrado and Caatinga biomes and transition between them. The third most affected were forests, of medium and large size, originating mainly in Atlantic Forest biome, but also present in transition areas between these, Cerrado and Caatinga.

This reduction in native vegetation formations and their substitution by areas for agricultural use caused a fall in tree cover (Table 10), both in P1 and in P2. As for the non-tree cover, in P1 and P2 there was an increase, reflecting the pasture and crop expansion in detriment of forest and savanna areas, medium to large vegetation. The bare soil, at the same time, was reduced in P1, even with native vegetation degradation, due to territorial growth of agricultural cover. Although there were dynamics similar to P1 in P2, that is, the replacement of native vegetation with pastures and crops, there was a significant increase in bare soil, in contrast to what happened in P1.

Table 10
Changes in tree and non-tree vegetable coverings and bare soil in the SFB.

Tree Cover (%)			**Non-Tree Cover (%)**			**Bare Soil (%)**		
MK Statistics	**P1**	**P2**	**MK Statistics**	**P1**	**P2**	**MK Statistics**	**P1**	**P2**
Average	-0.06	-0.2	Average	0.2	0.1	Average	-0.13	0.1
Min.	-0.56	-0.58	Min.	-0.28	-0.44	Min.	-0.6	-0.58
Max.	0.56	0.56	Max.	0.67	0.67	Max.	0.51	0.51
Std. Dev.	0.21	0.18	Std. Dev.	0.18	0.23	Std. Dev.	0.21	0.17
MK Range (P1)	**Area (%)**		**MK Range (P1)**	**Area (%)**		**MK Range (P1)**	**Area (%)**	
-0.56 to 0	60		-0.28 to 0	15		-0.6 to 0	73	
0 to 0.56	40		0 to 0.67	85		0 to 0.51	27	
MK Range (P2)	**Area (%)**		**MK Range (P2)**	**Area (%)**		**MK Range (P2)**	**Area (%)**	
-0.58 to 0	87		-0.44 to 0	36		-0.58 to 0	30	
0 to 0.56	13		0 to 0.67	64		0 to 0.51	70	

Between 1982 and 2014, in P1, tree cover reduced, on average, from 18.5–15%, and non-tree cover increased from 77.1–81.3%. Bare soil fell from 5.8–4%. In P2, tree cover dropped, on average, from 22–13.3%, and non-tree cover increased from 72.7–76.8%. Bare soil rose from 5.3–9.9%.

Concerning the NDVI (Table 11), even with drop in tree cover in P1, there was mostly an increase, which on average rose 0.06, from 0.50 to 0.56. In P2, in general, it remained stable, with a drop of 0.01, from 0.52 to 0.51, approximately half of the area falling and the remainder rising.

Table 11
Changes in NDVI in SFB.

MK Statistics	**P1**	**MK Statistics**	**P2**
Average	0.18	Average	0
Min.	-0.32	Min.	-0.35
Max.	0.56	Max.	0.56
Std. Dev.	0.17	Std. Dev.	0.13
MK Range (P1)	**Area (%)**	**MK Range (P2)**	**Area (%)**
-0.32 to 0	18	-0.35 to 0	57
0 to 0.56	82	0 to 0.56	43

The tests by Pettitt and Buishand (Fig. 5), show that the break in homogeneity in historical series of land use and land cover occurred in the late 1990s for P1 and early 2000s for P2, very close to the results achieved for variables from the previous subtopic.

4.3 Impacts and changes in São Francisco river' flow rate dynamics

Although the drop in rainfall index in P1 was small, 5% between 1948 and 2019, the drought events of the last decade (2010–2019) affected the permanence flow curve of São Francisco river (Q_{95} and Q_{50}) (Fig. 6). It is also noteworthy that these flows were influenced by the temporal behavior of rainfall, increasing when rainfall increases (between 1950 and 1989) and decreasing when rainfall drops (between 1990 and 2019).

Another relevant factor is the change in land cover caused by the expansion of activities and land uses, mainly linked to agriculture and livestock. Even though in P1 there was a fall in bare soils, this was accompanied by a reduction in tree vegetation cover and an increase in the non-tree vegetation cover, due exactly to increase in pastures and crops areas. This fact has implications for other variables related to energy flow and water cycle, such as the greater flow of radiation and, consequently, of heat, causing a greater evapotranspiration process, in addition to reduction in tree cover contribute to increase in surface

runoff and reduction of water soil infiltration, reducing subsurface runoff and soil moisture in plants root zone.

Even with the reduction in rainfall during the 2000s and 2010s, surface runoff was greater than in previous decades, when there were similar or higher rainfall levels. This has an impact on the long-term flow rate of São Francisco river, given the precipitated water that drains superficially is reaching the watercourses faster due to reduction of friction caused by the replacement of the land cover. Thus, water soil infiltration reduced and caused less subsurface runoff, impairing the recharge of groundwater that supplies tributaries and the main river itself. This supply is even more important in drought periods.

In P2 (Fig. 7), the situation is similar to P1, although there was a greater drop in tree cover and a greater increase in bare soil. The exception is the behavior of rainfall over the decades, which is not similar to that of flows rate (Fig. 7). This occurs because in P2 the flow rate also follows the behavior of P1 rains, which are responsible for 65% of the water entering basin on average.

The impacts are even clearer when the statistical results referring to the maximum, average and minimum flows rate are revealed, which show downward trends (MK) with values of -0.102, -0.109 and − 0.084 respectively, in P1 (Fig. 6), and P2 (Fig. 7) with values of -0.151, -0.062 and − 0.115. KPSS tests for all flows rate show that the critical levels have been reached, reporting non-stationarity in the series. The tests by Pettitt and Buishand reveal that the break in historical series homogeneity occurred in the early 2000s, in agreement with years obtained for data on land use and land cover and very close to energy flow and water cycle variables. This fact is a strong indication that changes in land use and land cover in SFB have resulted in changes in the natural cycles of energy and water in basin.

It is also worth mentioning another factor that influenced the flows rate, which is the construction of the Sobradinho dam, in the state of Bahia. Inaugurated in 1982, from then on the dam contributed to regularization of the São Francisco flow rate. Between 1959 and 1980, in rainy season, maximum and minimum flows rate reached values close to 4,600 and 2,800 m^3/s, respectively, and 1,200 and 1,100 m^3/s, respectively, in drought period. From the 1980s to 2000s, even with a certain increase in rainfall, maximum and minimum flows rate did not reach 3,600 and 2,400 m^3/s, respectively, in rainy season, and exceeded 1,900 and 1,500 m^3/s, respectively, in drought period, showing a control of increase in flows rate when the rains occur with greater frequency and intensity, and release when the drought occurs (Fig. 8).

The flow rate regularization shown in the fluviometric station located in P2 does not occur in the one located in P1, which reveals that there was a clear drop in the maximum and minimum flows rate over the three periods evaluated, except for some similar values that occur between the periods, notably in dry season. Comparing P2 to P1, the amplitude of maximum and minimum flows rate between rainy and drought periods in 2001–2019, shows how the dams can help to regulate water flow rate in watercourses and keep their availability even higher in drought periods.

In P2, despite the reduction in rainfall between 2001 and 2019, there was an average drop of 28% and 8% in maximum and minimum flows rate, respectively. In P1, the fall was 82% and 63%, respectively. This fact shows that without the construction of the dam, the situation in P2, regarding water availability in São Francisco river, could have been more serious in drought periods.

In 2001–2019 period, in addition to a small reduction in rainfall in P1 and a stable situation in P2, there was also an increase in average evapotranspiration in rainy season and a reduction in drought in both areas (Table 12). There was an increase in average surface runoff practically throughout the year, notably in greatest rainfall period, and average subsurface runoff decreased, mainly in rainy season in P1. The presence of moisture in plants' root zone also dropped in the period 2001–2019, in both areas. The average reduction of 5% of rainfall in P1 is one of the factors related to the reduction of water present in basin, but the increase in evapotranspiration and surface runoff, caused by changes in land cover, had a greater impact on water maintenance.

Table 12
Seasonal variation of water flow in SFB between 1951–1980 and 2001–2019.

Variable	**Average Variation (P1)**			
	Rainy Season		**Dry Season**	
	Absolute	**Relative**	**Absolute**	**Relative**
Rainf	-131 mm	-11%	-27 mm	-11%
Evap	+ 81 mm	+ 14%	-29 mm	-10%
Qs	+ 8.4 mm	+ 105%	+ 0.4 mm	+ 80%
Qsb	-201 mm	-55%	-2 mm	-7%
RootMoist	-152 mm	-9%	-146 mm	-12%
Variable	**Average Variation (P2)**			
	Rainy Season		**Dry Season**	
	Absolute	**Relative**	**Absolute**	**Relative**
Rainf	0 mm	0%	+ 26 mm	+ 16%
Evap	+ 33 mm	+ 7%	-47 mm	-19%
Qs	+ 102 mm	+ 3,792%	+ 24 mm	+ 2,380%
Qsb	-5 mm	-36%	-3 mm	-38%
RootMoist	-230 mm	-17%	-203 mm	-18%

The correlation (R) between the monthly data from January 1981 to December 2019 of NDVI with those of rain, evapotranspiration, root zone soil moisture of the plants, surface and subsurface runoff, shows, to a certain extent, the influence of vegetation maintaining humidity in basin.

Figure 9 shows how the NDVI has a higher correlation with rain, evapotranspiration and soil moisture in root zone. In other words, it shows how the seasonality of rainfall influences the seasonality of vegetation, with vegetation increasing its vigor in the rainy seasons and decreasing in the dry seasons, expect for some areas, probably influenced by local factors, such as relief, irrigation, among others.

The same occurs with soil moisture in root zone and with evapotranspiration, as in the rainy seasons it tends to have a greater water accumulation in the soil, increasing its humidity, and consequently a greater plant development, which also increases evapotranspiration processes. In the dry seasons, the lower occurrence of rain decreases inlet of water into basin, and with increase in energy flow (radiation and heat), it tends to increase potential evapotranspiration, removing more water from the system by this process.

Although NDVI shows the vigor and health status of vegetation with some success, there is some difficulty in defining its size, as there is no direct relationship between this and the values of this index, depending a lot on the type of vegetation evaluated, in which biome and climatic caracteristics is located. For this reason, this index obtained lower correlations with surface and subsurface runoff, which will vary according to the occurrence of precipitation. It also depends on the relief and obstacles that favor or not water infiltration in soil and flow speed on the surface, with plant sizes as important factors in this case. Land covers (bare soil, arboreal and non-arboreal vegetation) were not used in this correlation because their information is of annual frequency, and it is not possible to assess the seasonality of the process, which is important in assessing the correlations, mainly due to the differences in the rainy and dry seasons.

Correlating average monthly flow rate of the fluviometric stations located in P1 and P2, with variables of rainfall, surface and subsurface runoff (Fig. 10), it is clear their importance in the flow rate dynamics over time. However, notably, as subsurface runoff is vital for maintaining flow rate, especially in droughts. This shows how the recharge of groundwater is essential during rainy periods, and this process has been hampered by changes in land cover (Fig. 11).

As seen earlier, Buishand and Pettitt tests show that the break in homogeneity for energy flow, water cycle and land cover variables, occurred in the late 1990s and early 2000s, similar, too, the result for these tests in the cases of flows rate in P1 and P2, which were between 2000 and 2002. Thus, concerning the pre and post-1990s periods, for the entire SFB, the average reduction in rainfall volume was 2%, from 958.9 to 940.5 mm per year, down 18.4 mm. While rainfall is stable, average evapotranspiration increased by 5% (+ 38.1 mm), surface runoff increased by 225% (+ 36 mm) and water infiltration in the soil decreased by 52% (-92.5 mm) (Fig. 11).

This means that in the period before the 1990s, from 100% of the water volume that entered the basin (precipitation), 79% returned to the atmosphere through evapotranspiration. In the current period, after the 1990s, this ratio is 85%. The loss through surface runoff was 2% and became 6%. In other words, there was a reduction in the water infiltration into the soil, which corresponded to 19% of the water volume, which entered the basin due to rains. This ratio has now dropped to 9% (Fig. 11).

4 Conclusions

In this research, the following conclusions were reached:

- The variables related to energy flow and water cycle have undergone changes between 1948 and 2019, which contribute to evapotranspiration and surface runoff processes increase, and reduction of water infiltration in the soil, with drops in subsurface runoff and in humidity of the plants' root zone;
- The flow rate of São Francisco river has been impacted by such changes, since the water contribution of subsurface runoff has decreased in both P1 and P2, notably in the first, an area that represents 65% of the water entering SFB due to rain;
- The São Francisco river flow rate have been impacted mainly by the drop in the contribution of P1 in the maintenance of basin's water resources, notably by the reduction in subsurface runoff of the last two decades, caused by the greater loss of water in surface runoff and evapotranspiration;
- In summary, the very activities that depend on greater water maintenance in the basin are those that promote water loss through surface runoff and evapotranspiration, reducing flow rates of São Francisco river, by decreasing the recharge of aquifers and soil moisture.

Declarations

Acknowledgments, Samples, and Data

This research was supported in part by a grant from the Coordenação de Aperfeiçoamento de Pessoal de Nível Superior (CAPES) – Finance Code 001, belonging to the Education Ministry of Brazil. The entire database was obtained from secondary sources, on the websites indicated in subtopic 2.2, and duly referenced. The authors have no conflicts of interest to declare.

References

Ala-aho, P., Soulsby, C., Wang, H., Tetzlaff, D., 2017. Integrated surface-subsurface model to investigate the role of groundwater in headwater catchment runoff generation: A minimalist approach to parameterisation. J. Hydrol. 547, 664–677. https://doi.org/10.1016/j.jhydrol.2017.02.023

Alcoforado de Moraes, M.M.G., Biewald, A., Carneiro, A.C.G., Souza da Silva, G.N., Popp, A., Lotze-Campen, H., 2018. The impact of global change on economic values of water for Public Irrigation Schemes at the

São Francisco River Basin in Brazil. Reg. Environ. Chang. 18, 1943–1955. https://doi.org/10.1007/s10113-018-1291-0

Barber, C., Lamontagne, J.R., Vogel, R.M., 2020. Improved estimators of correlation and R^2 for skewed hydrologic data. Hydrol. Sci. J. 65, 87–101. https://doi.org/10.1080/02626667.2019.1686639

Beaudoing, H., Rodell, M., 2019. GLDAS Noah Land Surface Model L4 monthly 0.25 x 0.25 degree V2.0, Greenbelt, Maryland, USA, Goddard Earth Sciences Data and Information Services Center (GES DISC) [WWW Document]. NASA/GSFC/HSL. https://doi.org/10.5067/9SQ1B3ZXP2C5

Bezerra, B.G., Silva, L.L., Santos e Silva, C.M., de Carvalho, G.G., 2019. Changes of precipitation extremes indices in São Francisco River Basin, Brazil from 1947 to 2012. Theor. Appl. Climatol. 135, 565–576. https://doi.org/10.1007/s00704-018-2396-6

Bickici Arikan, B., Kahya, E., 2019. Homogeneity revisited: analysis of updated precipitation series in Turkey. Theor. Appl. Climatol. 135, 211–220. https://doi.org/10.1007/s00704-018-2368-x

Buishand, T.A., 1982. Some methods for testing the homogeneity of rainfall records. J. Hydrol. 58, 11–27. https://doi.org/10.1016/0022-1694(82)90066-X

Correia, R.C., Araújo, J.L.P., Cavalcanti, E. de B., 2001. A fruticultura como vetor de desenvolvimento: o caso dos municipios de Petrolina (PE) e Juazeiro (BA). - Portal Embrapa, in: Correia, R.C. (Embrapa S.-C., Araujo, J.L.P. (Embrapa S.-C. (Eds.), CONGRESSO BRASILEIRO DE ECONOMIA E SOCIOLOGIA RURAL. SOBER/ESALQ/EMBRAPA/UFPE/URFPE, Recife, Brasil, p. 8.

Creech, C.T., Siqueira, R.B., Selegean, J.P., Miller, C., 2015. Anthropogenic impacts to the sediment budget of São Francisco River navigation channel using SWAT. Int. J. Agric. Biol. Eng. 8, 1–20. https://doi.org/10.3965/j.ijabe.20150803.1372

Das, P., Behera, M.D., Patidar, N., Sahoo, B., Tripathi, P., Behera, P.R., Srivastava, S.K., Roy, P.S., Thakur, P., Agrawal, S.P., Krishnamurthy, Y.V.N., 2018. Impact of LULC change on the runoff, base flow and evapotranspiration dynamics in eastern Indian river basins during 1985–2005 using variable infiltration capacity approach. J. Earth Syst. Sci. 127, 19. https://doi.org/10.1007/s12040-018-0921-8

de Jong, P., Tanajura, C.A.S., Sánchez, A.S., Dargaville, R., Kiperstok, A., Torres, E.A., 2018. Hydroelectric production from Brazil's São Francisco River could cease due to climate change and inter-annual variability. Sci. Total Environ. 634, 1540–1553. https://doi.org/10.1016/j.scitotenv.2018.03.256

Didan, K., Barreto, A., 2016. NASA MEaSUREs Vegetation Index and Phenology (VIP) Vegetation Indices Monthly Global 0.05Deg CMG [Data set] [WWW Document]. NASA EOSDIS L. Process. DAAC. https://doi.org/10.5067/MEaSUREs/VIP/VIP30.004

Eastman, J.R., 2016. Terrset: Geospatial Monitoring and Modeling System Manual [WWW Document]. Clark Univ. URL https://clarklabs.org/wp-content/uploads/2016/10/Terrset-Manual.pdf (accessed 9.10.20).

Hansen, M., Song, X.P., 2018. Vegetation Continuous Fields (VCF) Yearly Global 0.05 Deg [Data set] [WWW Document]. NASA EOSDIS L. Process. DAAC. https://doi.org/10.5067/MEaSUREs/VCF/VCF5KYR.001

Hirsch, R.M., Slack, J.R., 1984. A Nonparametric Trend Test for Seasonal Data With Serial Dependence. Water Resour. Res. 20, 727–732. https://doi.org/10.1029/WR020i006p00727

Hirsch, R.M., Slack, J.R., Smith, R.A., 1982. Techniques of trend analysis for monthly water quality data. Water Resour. Res. 18, 107–121. https://doi.org/10.1029/WR018i001p00107

Jiang, S., Wei, L., Ren, L., Xu, C.Y., Zhong, F., Wang, M., Zhang, L., Yuan, F., Liu, Y., 2021. Utility of integrated IMERG precipitation and GLEAM potential evapotranspiration products for drought monitoring over mainland China. Atmos. Res. 247, 105141. https://doi.org/10.1016/j.atmosres.2020.105141

Kendall, M., 1975. Multivariate analysis. Charles Griffim & Company Ltd., London.

Koch, H., Biewald, A., Liersch, S., Azevedo, J.R.G. de, Silva, G.N.S. da, Kölling, K., Fischer, P., Koch, R., Hattermann, F.F., 2015. Scenarios of climate and land-use change,water demand and water availability for the São Francisco River basin. Rev. Bras. Ciências Ambient. 96–114. https://doi.org/10.5327/z2176-947820151007

Kwiatkowski, D., Phillips, P.C.B., Schmidt, P., Shin, Y., 1992. Testing the null hypothesis of stationarity against the alternative of a unit root. How sure are we that economic time series have a unit root? J. Econom. 54, 159–178. https://doi.org/10.1016/0304-4076(92)90104-Y

Lindsey, R., 2009. Climate and Earth's Energy Budget.

Mann, H.B., 1945. Nonparametric Tests Against Trend. Econometrica 13, 245. https://doi.org/10.2307/1907187

Mokhtari, A., Noory, H., Vazifedoust, M., 2018. Performance of Different Surface Incoming Solar Radiation Models and Their Impacts on Reference Evapotranspiration. Water Resour. Manag. 32, 3053–3070. https://doi.org/10.1007/s11269-018-1974-9

Pereira, S.B., Pruski, F.F., Da Silva, D.D., Ramos, M.M., 2007. Study of the hydrological behavior of São Francisco River and its main tributaries. Rev. Bras. Eng. Agric. e Ambient. 11, 615–622. https://doi.org/10.1590/S1415-43662007000600010

Pettitt, A.N., 1979. A Non-Parametric Approach to the Change-Point Problem. Appl. Stat. 28, 126. https://doi.org/10.2307/2346729

Pruski, F.F., Pereira, S.B., Novaes, L.F. de, Silva, D.D. da, Ramos, M.M., 2004. Specific yield discharge and mean precipitation in São Francisco Basin. Rev. Bras. Eng. Agrícola e Ambient. 8, 247–253. https://doi.org/10.1590/s1415-43662004000200013

Rodell, M., Houser, P.R., Jambor, U., Gottschalck, J., Mitchell, K., Meng, C.J., Arsenault, K., Cosgrove, B., Radakovich, J., Bosilovich, M., Entin, J.K., Walker, J.P., Lohmann, D., Toll, D., 2004. The Global Land Data Assimilation System. Bull. Am. Meteorol. Soc. 85, 381–394. https://doi.org/10.1175/BAMS-85-3-381

Rougé, C., Ge, Y., Cai, X., 2013. Detecting gradual and abrupt changes in hydrological records. Adv. Water Resour. 53, 33–44. https://doi.org/10.1016/j.advwatres.2012.09.008

Serinaldi, F., Kilsby, C.G., 2015. Stationarity is undead: Uncertainty dominates the distribution of extremes. Adv. Water Resour. 77, 17–36. https://doi.org/10.1016/j.advwatres.2014.12.013

Serinaldi, F., Kilsby, C.G., Lombardo, F., 2018. Untenable nonstationarity: An assessment of the fitness for purpose of trend tests in hydrology. Adv. Water Resour. 111, 132–155. https://doi.org/10.1016/j.advwatres.2017.10.015

Seyoum, W.M., Milewski, A.M., 2017. Improved methods for estimating local terrestrial water dynamics from GRACE in the Northern High Plains. Adv. Water Resour. 110, 279–290. https://doi.org/10.1016/j.advwatres.2017.10.021

Souza, C.M., Z. Shimbo, J., Rosa, M.R., Parente, L.L., A. Alencar, A., Rudorff, B.F.T., Hasenack, H., Matsumoto, M., G. Ferreira, L., Souza-Filho, P.W.M., de Oliveira, S.W., Rocha, W.F., Fonseca, A. V., Marques, C.B., Diniz, C.G., Costa, D., Monteiro, D., Rosa, E.R., Vélez-Martin, E., Weber, E.J., Lenti, F.E.B., Paternost, F.F., Pareyn, F.G.C., Siqueira, J. V., Viera, J.L., Neto, L.C.F., Saraiva, M.M., Sales, M.H., Salgado, M.P.G., Vasconcelos, R., Galano, S., Mesquita, V. V., Azevedo, T., 2020. Reconstructing Three Decades of Land Use and Land Cover Changes in Brazilian Biomes with Landsat Archive and Earth Engine. Remote Sens. 12, 2735. https://doi.org/10.3390/rs12172735

Sun, T., Ferreira, V., He, X., Andam-Akorful, S., 2016. Water Availability of São Francisco River Basin Based on a Space-Borne Geodetic Sensor. Water 8, 213. https://doi.org/10.3390/w8050213

Torres, M.D.O., Maneta, M., Howitt, R., Vosti, S.A., Wallender, W.W., Bassoi, L.H., Rodrigues, L.N., 2012. Economic impacts of regional water scarcity in the São Francisco river Basin, Brazil: An application of a linked hydro-economic model. Environ. Dev. Econ. 17, 227–248. https://doi.org/10.1017/S1355770X11000362

Umair, M., Kim, D., Choi, M., 2019. Impacts of land use/land cover on runoff and energy budgets in an East Asia ecosystem from remotely sensed data in a community land model. Sci. Total Environ. 684, 641–656. https://doi.org/10.1016/j.scitotenv.2019.05.244

Yan, G., Jiao, Z.H., Wang, T., Mu, X., 2020. Modeling surface longwave radiation over high-relief terrain. Remote Sens. Environ. 237, 111556. https://doi.org/10.1016/j.rse.2019.111556

Yang, F., Lu, H., Yang, K., He, J., Wang, W., Wright, J.S., Li, C., Han, M., Li, Y., 2017. Evaluation of multiple forcing data sets for precipitation and shortwave radiation over major land areas of China. Hydrol. Earth Syst. Sci. 21, 5805–5821. https://doi.org/10.5194/hess-21-5805-2017

Yin, L., Feng, X., Fu, B., Chen, Y., Wang, X., Tao, F., 2020. Irrigation water consumption of irrigated cropland and its dominant factor in China from 1982 to 2015. Adv. Water Resour. 143, 103661. https://doi.org/10.1016/j.advwatres.2020.103661

Yozgatligil, C., Yazici, C., 2016. Comparison of homogeneity tests for temperature using a simulation study. Int. J. Climatol. 36, 62–81. https://doi.org/10.1002/joc.4329

Yuan, R.Q., Chang, L.L., Gupta, H., Niu, G.Y., 2019. Climatic forcing for recent significant terrestrial drying and wetting. Adv. Water Resour. 133, 103425. https://doi.org/10.1016/j.advwatres.2019.103425

Figures

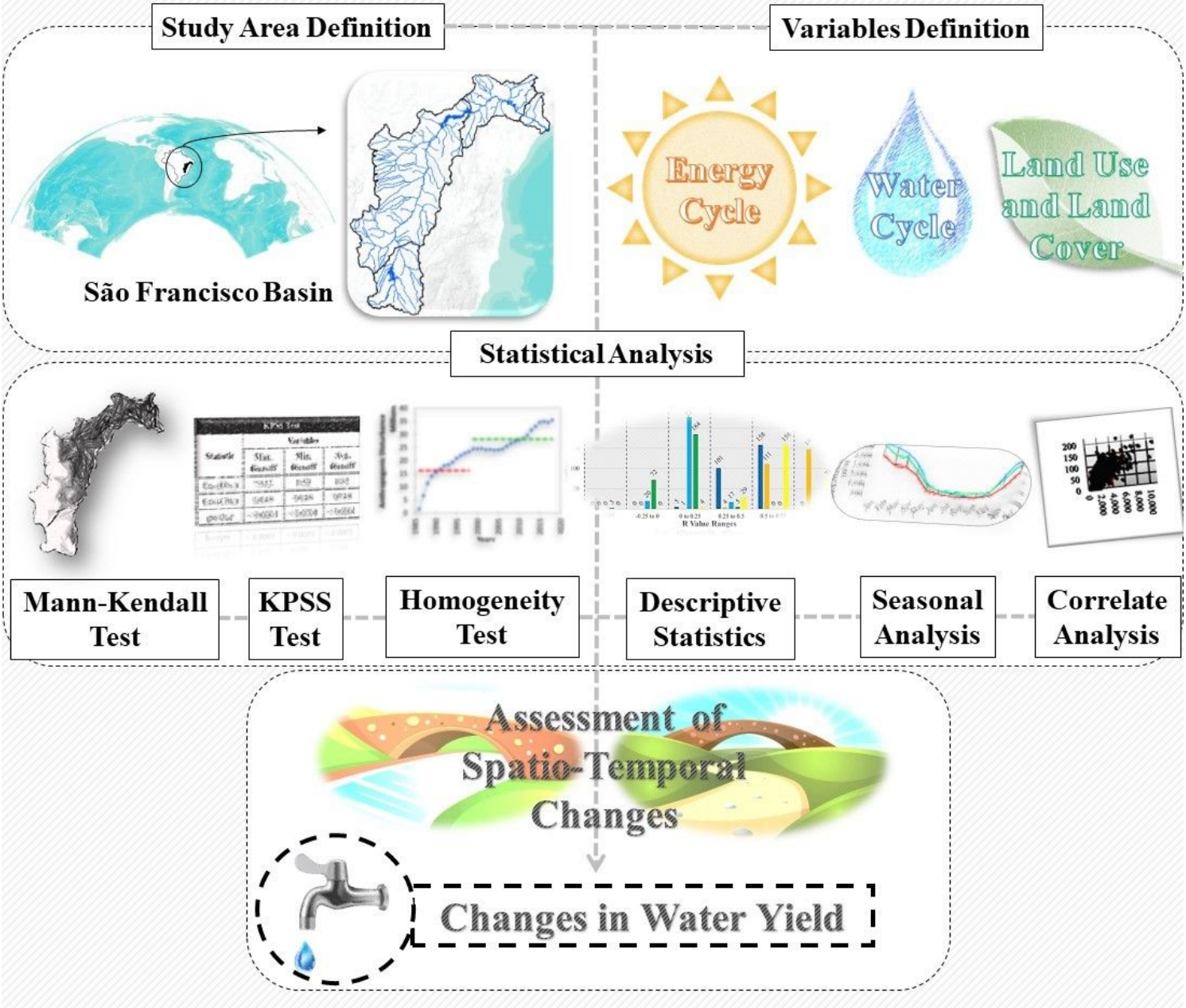

Figure 1

Methodological flowchart

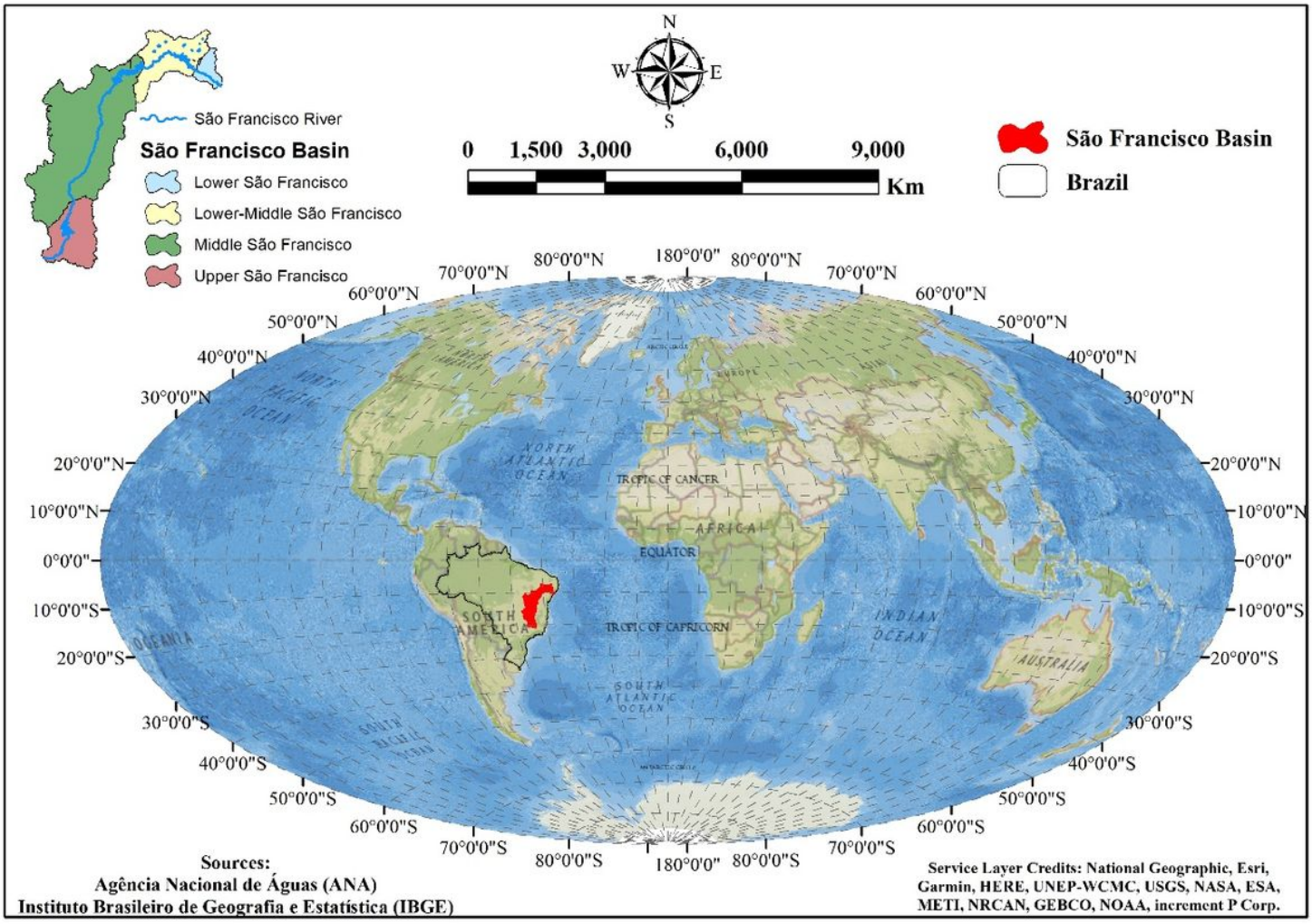

Figure 2

Study area location. Note: The designations employed and the presentation of the material on this map do not imply the expression of any opinion whatsoever on the part of Research Square concerning the legal status of any country, territory, city or area or of its authorities, or concerning the delimitation of its frontiers or boundaries. This map has been provided by the authors.

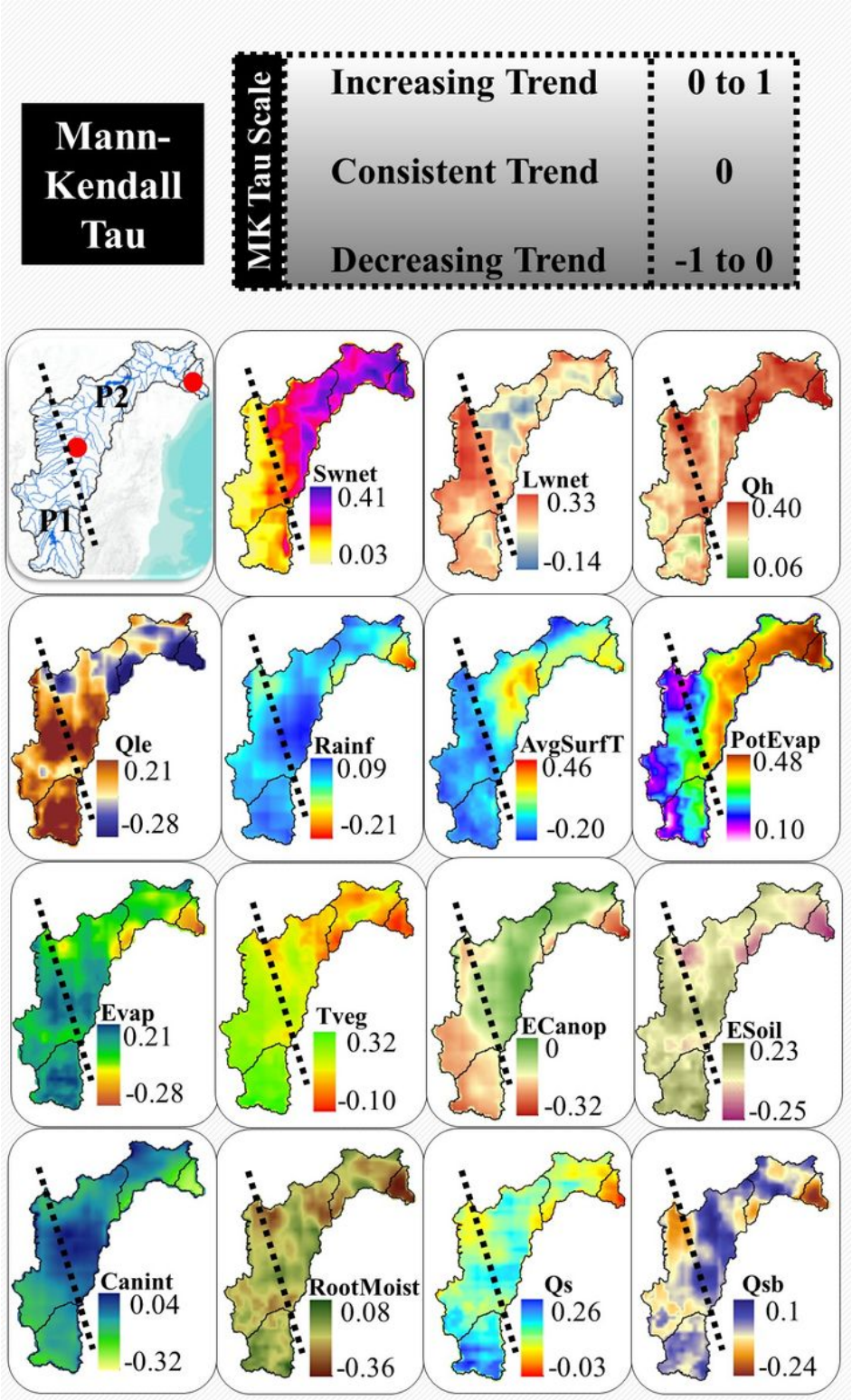

Figure 3

Trends in variables referring to energy flow and water cycle in SFB between January 1948 and December 2019. The red dots are the fluviometric stations locations with codes 45298000 (P1) and 49705000 (P2). Note: The designations employed and the presentation of the material on this map do not imply the expression of any opinion whatsoever on the part of Research Square concerning the legal status of any

country, territory, city or area or of its authorities, or concerning the delimitation of its frontiers or boundaries. This map has been provided by the authors.

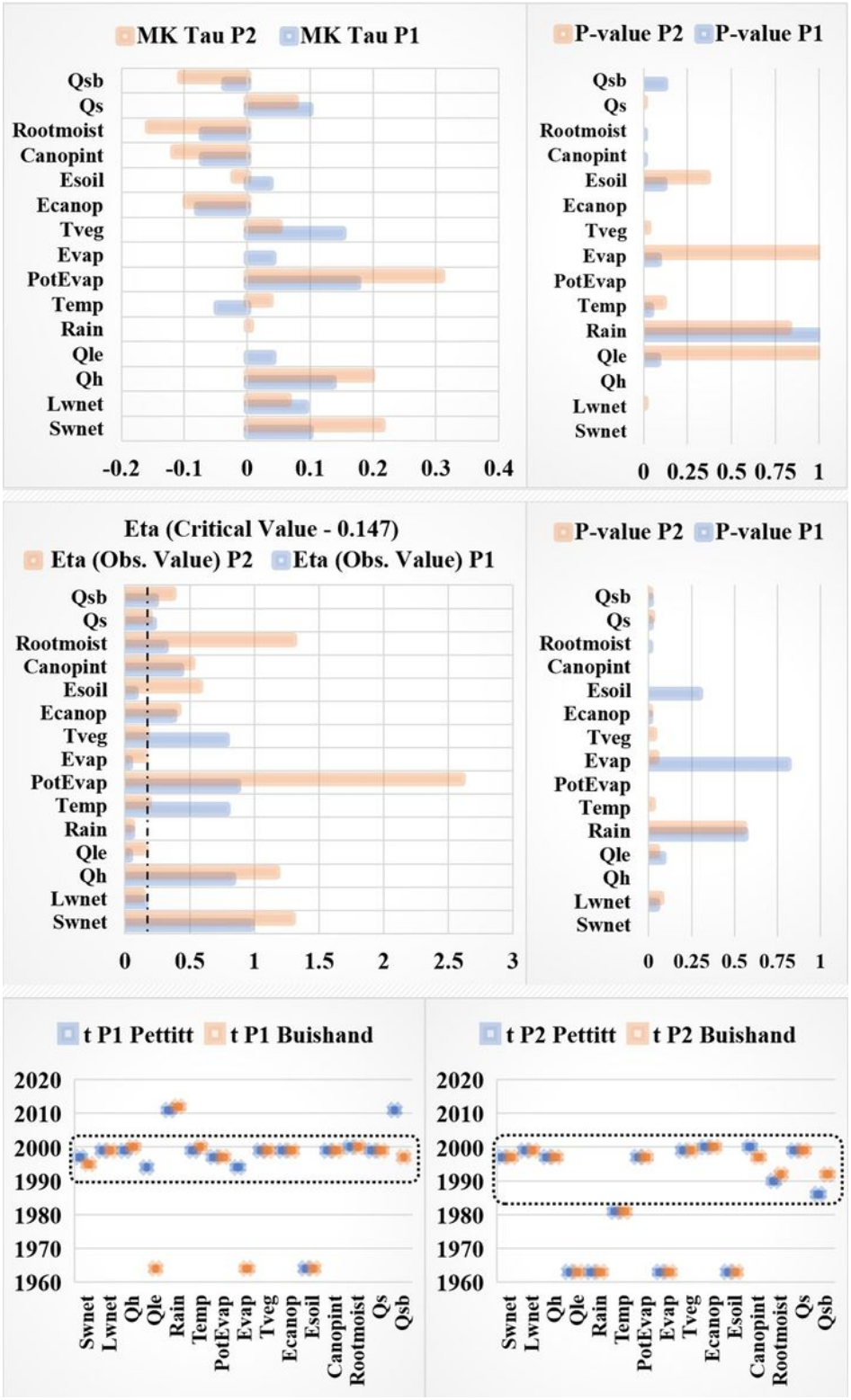

Figure 4

Mann-Kendall, KPSS and Homogeneity tests (Pettitt and Buishand) for energy flow and water cycle variables in SFB.

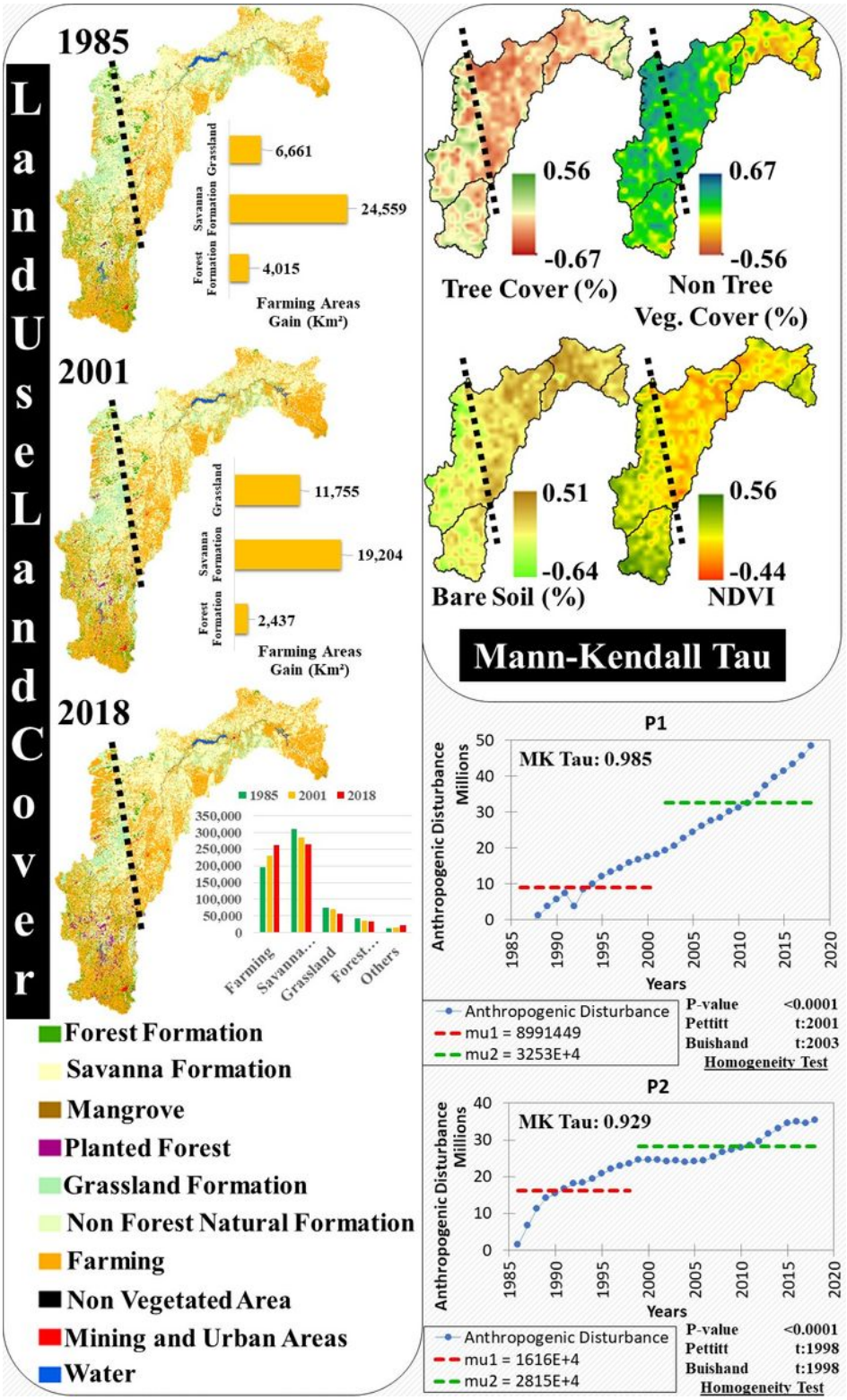

Figure 5

Changes in land use and land cover in SFB and its effects on the presence of tree and non-tree vegetation cover and bare soil. Note: The designations employed and the presentation of the material on this map do not imply the expression of any opinion whatsoever on the part of Research Square concerning the legal status of any country, territory, city or area or of its authorities, or concerning the delimitation of its frontiers or boundaries. This map has been provided by the authors.

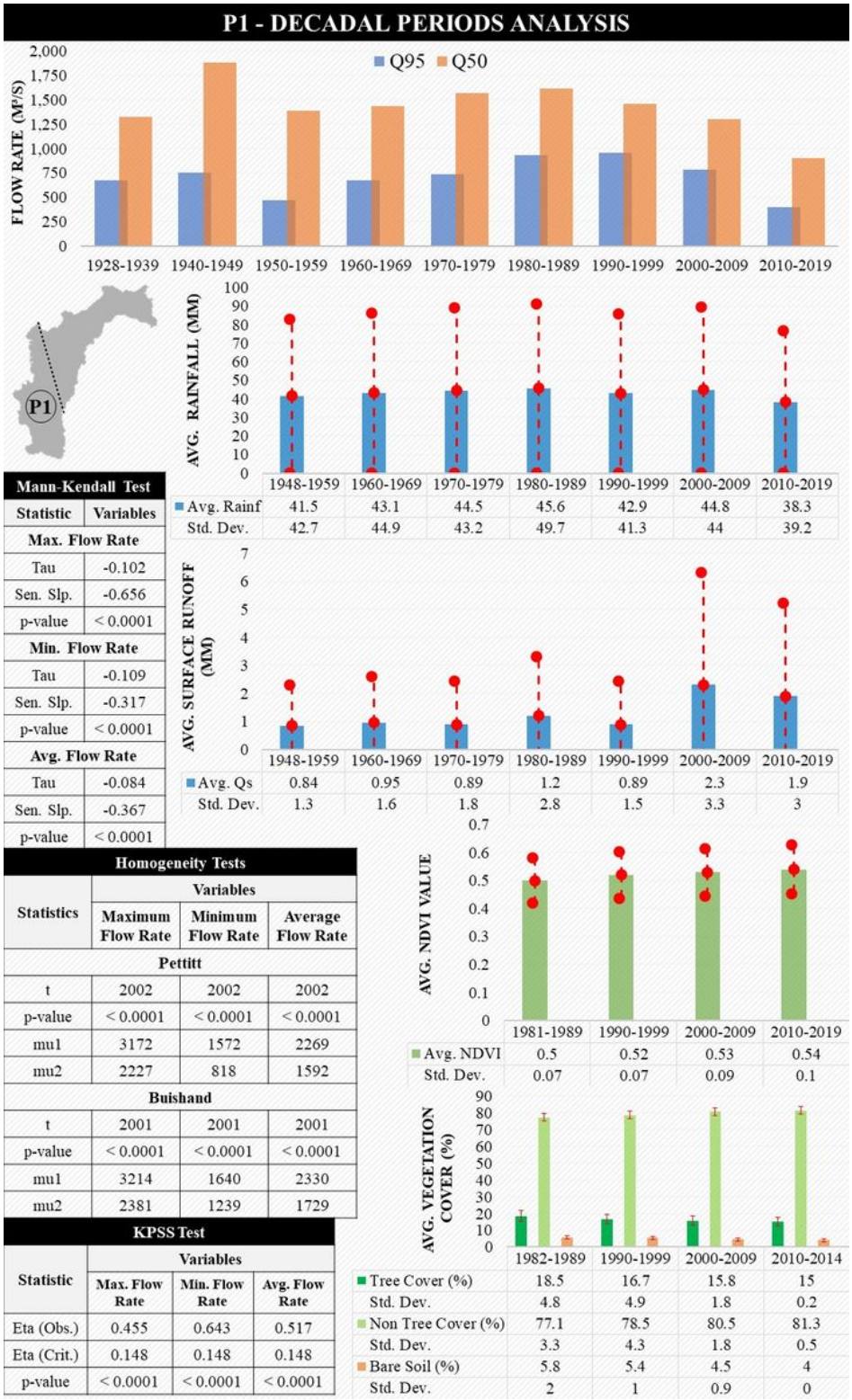

Mann-Kendall Test	
Statistic	Variables
Max. Flow Rate	
Tau	-0.102
Sen. Slp.	-0.656
p-value	< 0.0001
Min. Flow Rate	
Tau	-0.109
Sen. Slp.	-0.317
p-value	< 0.0001
Avg. Flow Rate	
Tau	-0.084
Sen. Slp.	-0.367
p-value	< 0.0001

Homogeneity Tests			
Statistics	Variables		
	Maximum Flow Rate	Minimum Flow Rate	Average Flow Rate
Pettitt			
t	2002	2002	2002
p-value	< 0.0001	< 0.0001	< 0.0001
mu1	3172	1572	2269
mu2	2227	818	1592
Buishand			
t	2001	2001	2001
p-value	< 0.0001	< 0.0001	< 0.0001
mu1	3214	1640	2330
mu2	2381	1239	1729

KPSS Test			
Statistic	Variables		
	Max. Flow Rate	Min. Flow Rate	Avg. Flow Rate
Eta (Obs.)	0.455	0.643	0.517
Eta (Crit.)	0.148	0.148	0.148
p-value	< 0.0001	< 0.0001	< 0.0001

Figure 6

Influence of rain dynamics and changes in land cover on the behavior of SFB flow rate in P1.

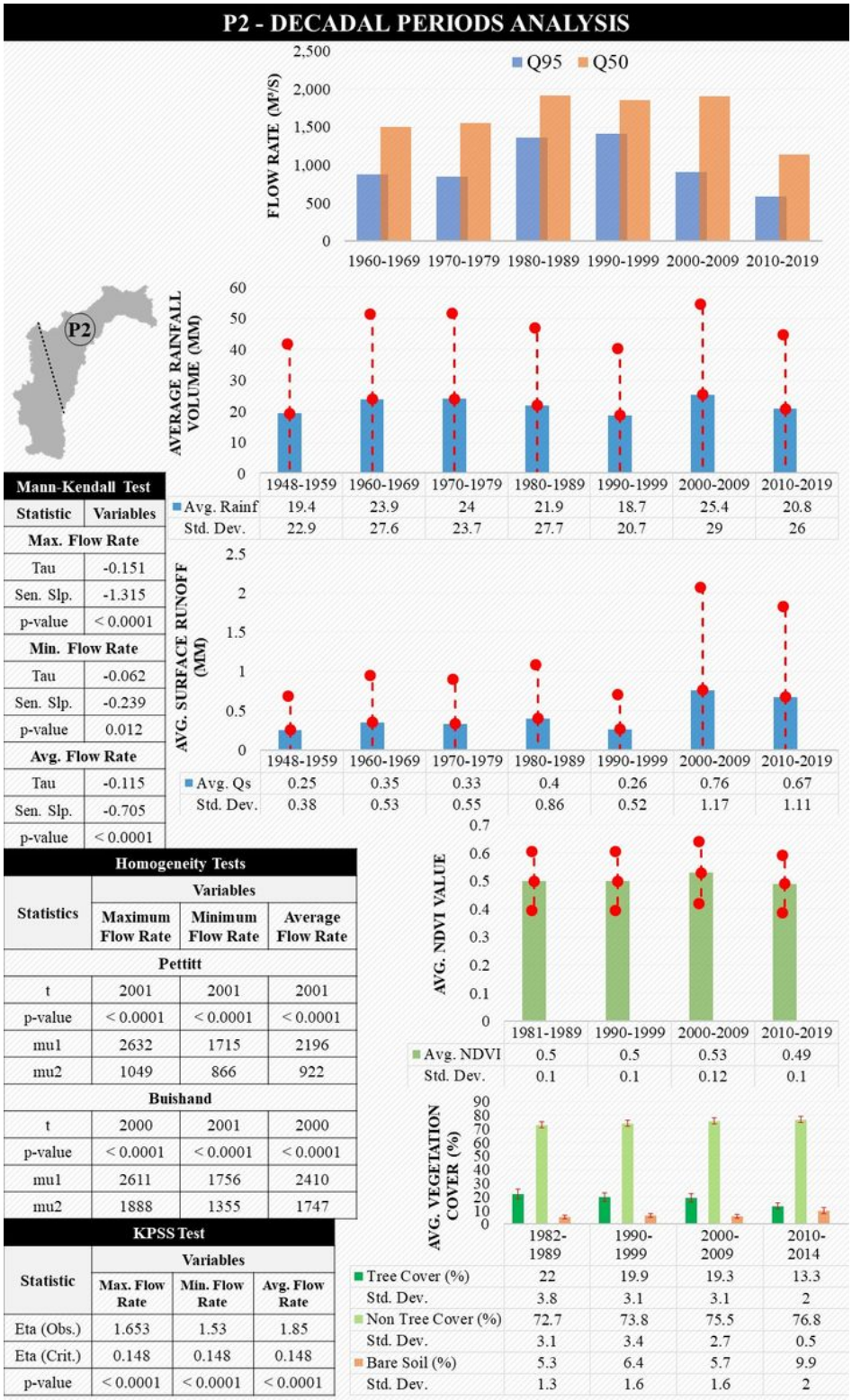

Mann-Kendall Test	
Statistic	**Variables**
Max. Flow Rate	
Tau	-0.151
Sen. Slp.	-1.315
p-value	< 0.0001
Min. Flow Rate	
Tau	-0.062
Sen. Slp.	-0.239
p-value	0.012
Avg. Flow Rate	
Tau	-0.115
Sen. Slp.	-0.705
p-value	< 0.0001

Homogeneity Tests			
Statistics	**Variables**		
	Maximum Flow Rate	**Minimum Flow Rate**	**Average Flow Rate**
Pettitt			
t	2001	2001	2001
p-value	< 0.0001	< 0.0001	< 0.0001
mu1	2632	1715	2196
mu2	1049	866	922
Buishand			
t	2000	2001	2000
p-value	< 0.0001	< 0.0001	< 0.0001
mu1	2611	1756	2410
mu2	1888	1355	1747

KPSS Test			
Statistic	**Variables**		
	Max. Flow Rate	**Min. Flow Rate**	**Avg. Flow Rate**
Eta (Obs.)	1.653	1.53	1.85
Eta (Crit.)	0.148	0.148	0.148
p-value	< 0.0001	< 0.0001	< 0.0001

Figure 7

Influence of rain dynamics and changes in land cover on the behavior of SFB flow rate in P2.

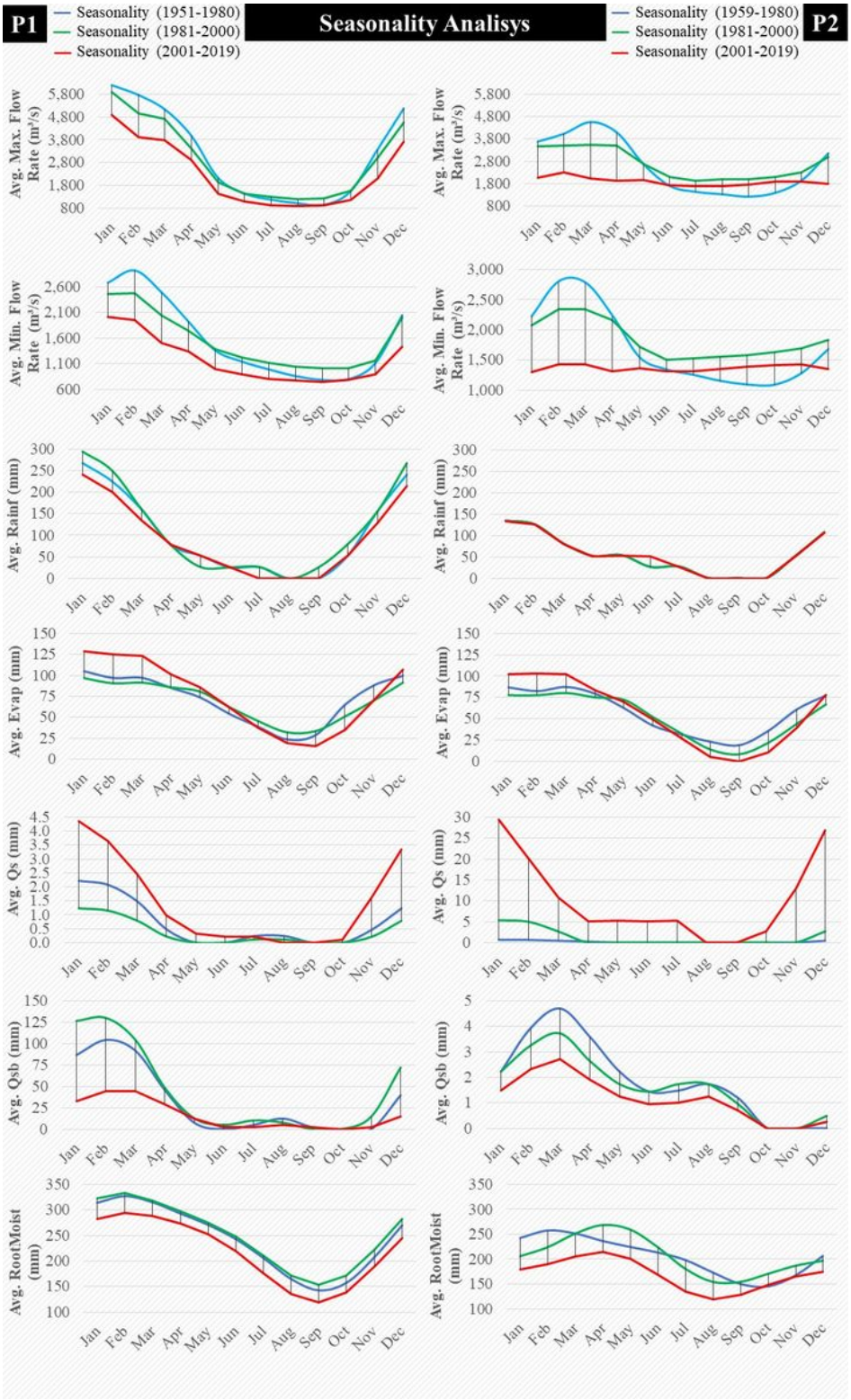

Figure 8

Seasonal analysis of variables related to water cycle in the SFB.

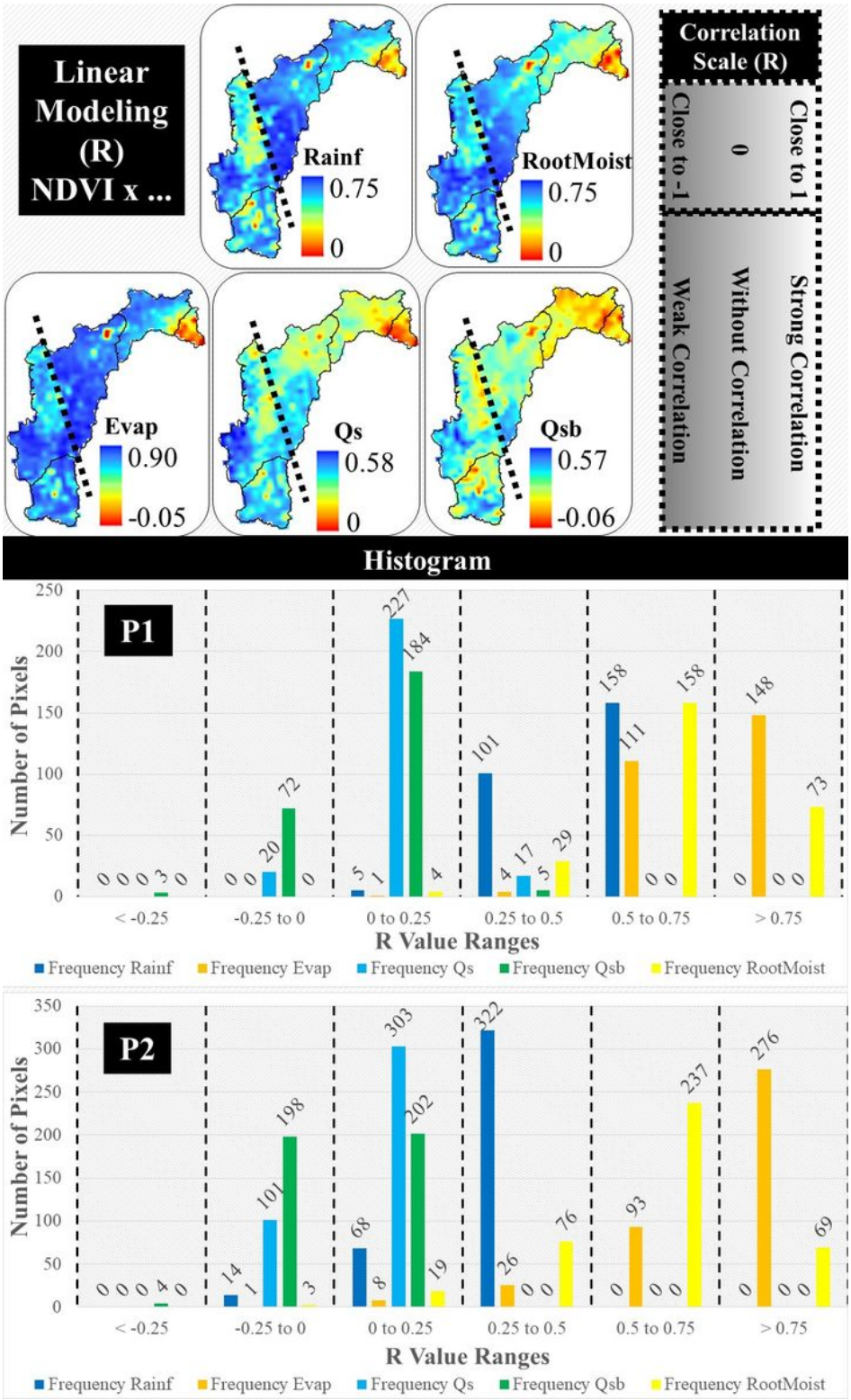

Figure 9

Correlations between NDVI and water cycle variables in SFB. Note: The designations employed and the presentation of the material on this map do not imply the expression of any opinion whatsoever on the part of Research Square concerning the legal status of any country, territory, city or area or of its authorities, or concerning the delimitation of its frontiers or boundaries. This map has been provided by the authors.

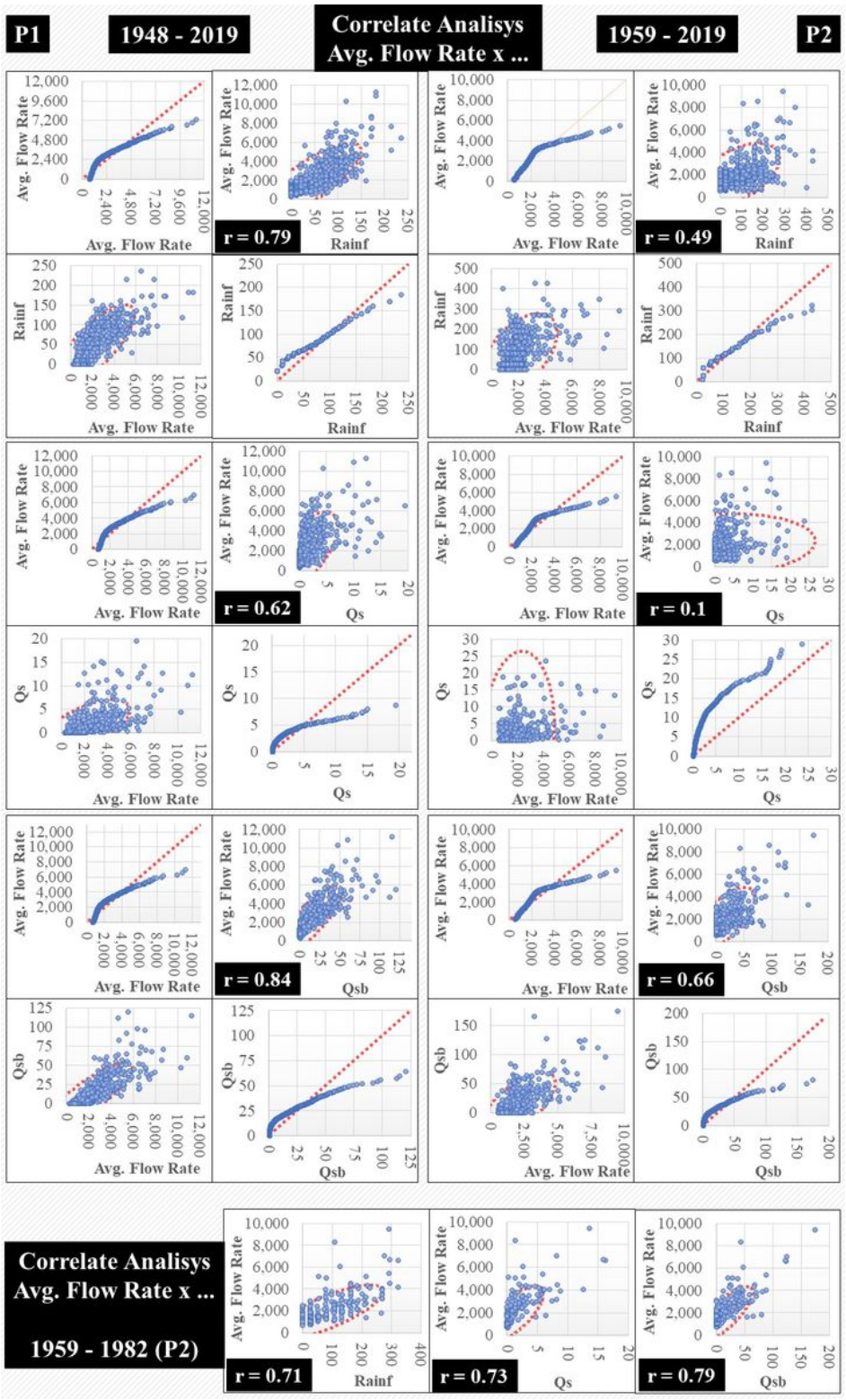

Figure 10

Correlations between average monthly flow rate with rainfall, surface and subsurface runoff data in SFB. Note: the construction of Sobradinho dam influenced the correlation values at the fluviometric station located in P2, due to flow rate regularization in São Francisco river, which significantly changed its behavior compared to other variables natural dynamics.

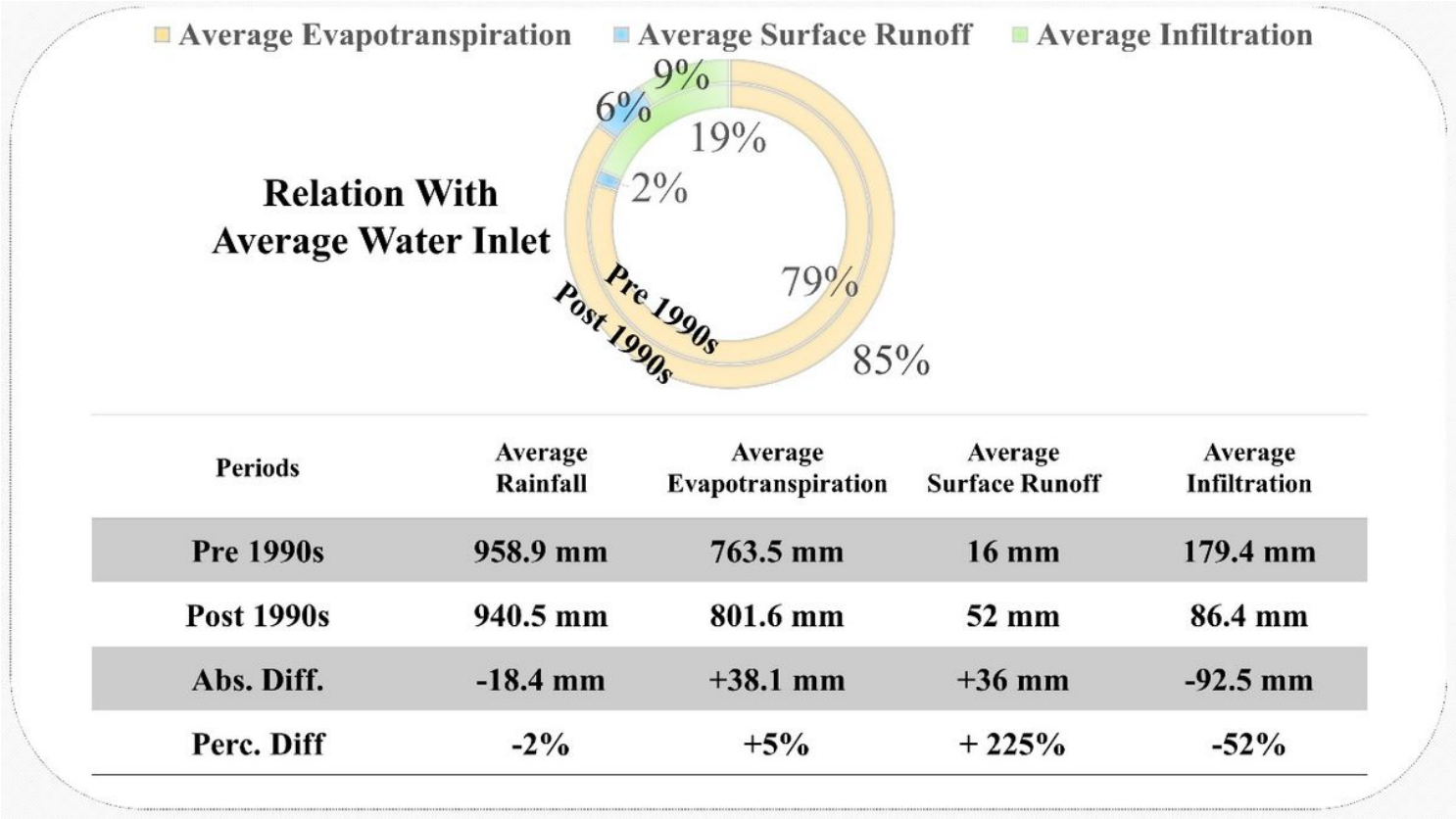

Periods	Average Rainfall	Average Evapotranspiration	Average Surface Runoff	Average Infiltration
Pre 1990s	958.9 mm	763.5 mm	16 mm	179.4 mm
Post 1990s	940.5 mm	801.6 mm	52 mm	86.4 mm
Abs. Diff.	-18.4 mm	+38.1 mm	+36 mm	-92.5 mm
Perc. Diff	-2%	+5%	+ 225%	-52%

Figure 11

Simplified water balance for the pre and post-1990s periods at SFB.